Low-Noise Detector of Minimally Ionizing Paricles Based On Microchannel Plates

N.A. Makarov[a],*, G.A. Feofilov[a], N.I. Kalinichenko[a], A. Kozhedub[a], V.N. Popov[a], F.F. Valiev[a] and A.K. Vlasnikov[a]

[a] *St. Petersburg State University, St. Petersburg, 199034 Russia*

**e-mail: n.a.makarov@spbu.ru*

Received April 10, 2025; revised September 10, 2025; accepted

Abstract — Detection of minimally ionizing particles in rare processes requires the creation of fast detectors with high efficiency and low noise levels. For a device consisting of two MCP assemblies, the possibility of increasing the detection efficiency of minimally ionizing particles (~95%) with a simultaneous increase in the signal-to-background ratio and with high resistance to electromagnetic interference is shown.

Keywords: rare event, minimally ionizing particle, fast detection system, nanosecond coincidence circuit, signal-to-background ratio

DOI:

Abstract —Efficient detection of minimally ionizing particles (MIPs) in rare physical processes requires fast detectors with high efficiency and low intrinsic noise. In this work, we present a detector based on a configuration of two microchannel plate (MCP) assemblies. This arrangement demonstrates a detection efficiency of approximately 95% for MIPs, while simultaneously enhancing the signal-to-background ratio and exhibiting strong resilience to electromagnetic interference. These results indicate that dual-MCP architectures offer a promising approach for high-precision, low-noise particle detection in challenging experimental environments.

INTRODUCTION

The NICA (Nuclotron-based Ion Collider fAcility) accelerator complex, currently under construction at the Joint Institute for Nuclear Research (Dubna, Russia), is designed to enable unique studies of baryon-rich matter in the MPD (MultiPurpose Detector [1,2]) experiment. It will employ high-intensity colliding ion beams (up to ^{79}Au) with an average luminosity of L=10^{27}cm^{-2}s^{-1} in the nucleon-energy range of 4–11 GeV/nucleon. The extensive and precise dataset expected from the MPD experiment will allow detailed investigations of the phase diagram of strongly interacting matter, including the exploration of possible deconfinement regions and the search for the critical point. Additionally, the SPD (Spin Physics Detector [3]) experiment aims to study the spin composition of nucleons and polarization phenomena in collisions of light and heavy ions, using polarized proton and deuteron beams with longitudinal and transverse polarization and luminosities up to $10^{32}\ \text{cm}^{-2} \cdot \text{s}^{-1}$.

Under the high-intensity beam conditions of the NICA collider, the primary experimental goal at the MPD and SPD facilities is to determine the initial conditions of each hadronic collision event. Rapid event selection requires precise information on the collision time (T0) [4,5], the interaction point (IP), suppression of events arising from interactions with residual gas in the ion guide, data on the reaction plane for each event, and determination of the collision centrality. Such measurements are crucial for subsequent physics analyses. Moreover, under realistic beam conditions, fast detectors must provide high sensitivity while maintaining immunity to electromagnetic interference in the microwave range.

To address the requirements for fast monitoring of high-intensity collisions at NICA, a Fast Beam-Beam Collision monitor (FBBC) was previously proposed [6], designed to operate in combination with a Beam Position Monitor (BPM) [7]. The FBBC detector is capable of monitoring collision intensity, determining the IP [8] and event time, and recording the azimuthal distribution and time-of-flight of the resulting charged particles. When implemented with microchannel plates (MCPs), the FBBC can also be used to analyze collision centrality. Previous studies [9–13] have demonstrated that event-by-event measurements of angular distributions and time-of-flight of charged particles, combined with machine learning techniques, allow the impact parameter of each heavy-ion collision to be determined with high precision (~1 fm).

Both the FBBC and BPM systems employ MCPs, which offer rapid response for charged particle detection. Their compatibility with ultra-high vacuum and the compactness of the BPM and FBBC components make them well-suited for installation in the NICA collider's vacuum beamline. The BPM system, based on residual gas ionization, provides high-precision, fast bunch-by-bunch beam position measurements. A two-coordinate MCP-based BPM profilometer was successfully implemented in 2021 [7] to monitor ion beams within the high-vacuum booster ring of the NICA accelerator complex. The FBBC detector may also be located outside the ion guide, within a separate vacuum system, utilizing a multi-anode readout to record particle time-of-flight and angular distributions for each event for short signals from the MCP detector.

The MCP detector consists of a chevron assembly of two microchannel plates with a defined microchannel orientation and an anode system (Fig. 1). For minimally ionizing particle detection, the first MCP plate functions as an active target, generating primary electrons and initiating an electron avalanche as charged particles traverse the plate. This avalanche induces a signal on the corresponding anode. The MCP detector provides a signal duration of less than 2 ns, with high temporal resolution (signal rise time < 800 ps, Fig. 2). MCP detectors also feature high gain (~10^6–10^7). However, the chevron MCP array produces a broad signal amplitude spectrum (Fig. 3), with low-amplitude noise pulses—so-called dark currents— usually rejected via thresholding. The rate of such background signals depends on MCP fabrication and accelerating voltage, ranging from ~1 to ~100 pulses/(s·cm²). Lowering the detection threshold to increase efficiency is limited by the concomitant rise in noise. Early measurements with minimally ionizing particle beams [14–16] yielded efficiencies of ~80%.

In this work, we propose a low-noise detector for minimally ionizing radiation within the FBBC system. The detector employs two sequential MCP assemblies with a differential signal pickup to suppress electromagnetic interference and a coincidence circuit to reduce background and enhance detection efficiency. The paper is structured as follows: Section 1 describes the design of the low-noise MCP-based detector for minimally ionizing radiation; Section 2 presents laboratory tests of the improved detector; and the final section summarizes the conclusions.

1. DEVICE DESCRIPTION

To ensure immunity to potential electromagnetic interference, a chevron-shaped MCP detector assembly with a differential signal pickup circuit was developed (Fig. 4). A key feature of this design is the detection of a differential signal: one from the anode and one from the lower surface of the second MCP (MCP-2) (Fig. 4). These signals are transmitted along a symmetric transmission line to the two inputs of a fast differential comparator.

When a charged particle traverses the MCP, it generates an electron avalanche that induces two signals of opposite polarity—one on the anode and one on the lower surface of MCP-2. These signals are transmitted via a 100 Ω symmetric transmission line to the differential input of the comparator, which then produces a logic output indicating particle detection. In-phase electromagnetic interference, appearing with the same polarity on both lines, does not generate a signal at the comparator output. The comparator features adjustable thresholds and low intrinsic noise, allowing the detection threshold to be reduced to approximately 5 mV.

To further improve detection efficiency and reduce background noise for minimally ionizing particles, the present design employs two identical chevron MCP assemblies arranged sequentially within a vacuum chamber *2* (Fig. 5). The first assembly *3*, with a flat anode *4*, is positioned at the upper part of the chamber, while the second MCP chevron assembly *10*, with a flat anode *11*, is located parallel to the first.

The anodes *4* and *11* of the two chevron assemblies are connected via signal transmission lines *5* and *12* to vacuum connectors *6* and *13*. Similarly, the surfaces of the MCPs nearest the anodes are connected via signal transmission lines *7* and *14* to vacuum connectors. Pairs of signals—from the flat anodes and the bottom MCP surfaces—are fed to fast comparators *8* and *15*. The comparator outputs are then connected to a nanosecond coincidence circuit *9*, which in turn is connected to a registration unit *1*. This unit records a signal only when a minimally ionizing particle passes through both chevron assemblies.

As a particle traverses the sequential MCP assemblies, it initiates primary ionization and the subsequent emission of secondary electrons from the MCP microchannel walls. These electrons are accelerated by the electric field between the ends of the MCP in each chevron assembly, with the potential difference between the bottom plane of the chevron MCP and the anode directing the avalanche toward the anode. This process induces signals on both the bottom conductive layer and the anode of each assembly. Signals with opposite polarity are transmitted via matched differential lines (100 Ω) through vacuum connectors to the comparator inputs. The coincidence circuit registers an event only when a particle passes through both MCP assemblies, effectively suppressing random noise in the low-amplitude region of the signal spectrum while reliably detecting true particle events. The registration block records the output of the coincidence circuit.

2. TEST RESULTS AND DISCUSSION

A prototype device was assembled, consisting of two identical chevron MCP assemblies, flat anodes, transmission lines, ADCMP604 fast comparators, a nanosecond coincidence circuit, and a registration unit implemented on an EPM240 FPGA. Each chevron MCP assembly comprises two standard MCPs with a diameter of 25 mm (active area diameter 20 mm), channel diameter of 6 μm, and resistance in the range of 100–300 MΩ. A flat anode of $10 \times 10\ \mathrm{mm}^2$ is positioned beneath each chevron assembly. The MCP assemblies are housed in an insulating FR4 fluoroplastic case, providing mechanical stability, defined geometry, and high-voltage insulation. High voltage is supplied to each assembly from an external voltage divider.

The anode of each chevron assembly is connected via a transmission line to a vacuum microwave output connector, which transmits the signal directly to the corresponding comparator input. The signal registration threshold is determined by the comparator threshold, which can be independently set for each channel. Comparator outputs are fed to a nanosecond coincidence circuit, whose output is connected to the registration unit. This unit records events corresponding to minimally ionizing charged particles passing through the device.

To suppress in-phase electromagnetic interference, a differential signal pickup is employed. In this scheme, two signals from chevron assembly—the direct signal and the inverted signal from the lower surface of MCP—are sent to the comparator input. The comparator output depends on the difference between these two signals. External electromagnetic interference induces identical pulses on both lines, which are effectively canceled by the comparator, ensuring robust detection even in the presence of external noise.

The prototype was mounted on a circular flange of a multifunctional vacuum chamber, which also houses vacuum connectors for signals and high-voltage connectors for the external divider. Estimates accounting for cosmic muon flux indicate that, for a coincidence circuit resolution of τ=50 ns, individual MCP noise rates of N_1=N_2=100 pulses/(s·cm²), and a comparator threshold of 10 mV, the expected rate of random coincidences does not exceed 5×10^{-4} pulses/(s·cm²). Experimental measurements were found to be consistent with these estimates.

The detection efficiency for minimally ionizing charged particles was evaluated using standard cosmic muon techniques. An additional MCP chevron assembly was incorporated into the setup to implement a triple-coincidence scheme. The efficiency ε was determined as the ratio of triple coincidences N_3 to double coincidences N_2:

$$\varepsilon=N_3/N_2,$$

where N_3 is the number of coincidences from all three assemblies, and N_2 is the number of coincidences from the two chevron assemblies of the device.

Using this method, the two-stage MCP assembly demonstrated a registration efficiency of 95±4% for minimally ionizing cosmic muons.

CONCLUSIONS

To enhance the efficiency of detecting minimally ionizing particles and improve the signal-to-noise ratio, a detector system based on two chevron MCP assemblies and a nanosecond coincidence circuit was developed and tested.

The implementation of a novel differential signal pickup scheme—collecting signals from both the anode and the lower surface of the second MCP in each chevron assembly—provides effective suppression of in-phase electromagnetic interference when combined with a fast differential comparator. Simultaneously, the coincidence circuit eliminates random noise pulses originating from individual MCP assemblies while reliably registering true signals from minimally ionizing particles traversing the detector.

As a result, the use of the nanosecond coincidence scheme enabled an increase in the registration efficiency for minimally ionizing particles to (95±4)%, accompanied by a background reduction of several orders of magnitude, down to approximately 10^{-3} pulses /(s·cm²).

FUNDING

This work was supported by ongoing institutional funding. The authors acknowledge Saint-Petersburg State University for a research project 103821868.

CONFLICT OF INTEREST

The authors of this work declare that they have no conflicts of interest.

REFERENCES

1. Abgaryan V., Acevedo Kado R., Afanasyev S.V., et al. (MPD Collaboration), *Eur. Phys. J. A*, 2022, vol. 58, p. 140. https://doi.org/10.1140/epja/s10050-022-00750-6
2. Abdulin R., Abgaryan Vahagn, Adhikary Rivu, et al. (MPD collaboration), *Revista Mexicana de Física*, 2025, vol. 71, p. 1. https://doi.org/10.31349/RevMexFis.71.041201
3. Abazov V., Abramov V., Afanasyev L., et al. (SPD Collaboration), *Natural Science Review*, 2024, vol. 1, no. 1, p. 1. https://doi.org/10.48550/arXiv.2404.08317
4. Valiev F.F., Vechernin V.V., and Feofilov G.A. *Bull. Russ. Acad. Sci. Phys.*, 2024, vol. 88, no. 8, p. 1312. https://doi.org/10.1134/s1062873824707499
5. Valiev F.F., Kalinichenko N.I., Makarov N.A., et al., *Bull. Russ. Acad. Sci. Phys.*, 2024, vol. 88, p. 1319. https://doi.org/10.1134/s1062873824707505
6. Baldin A.A., Feofilov G.A., Har'yuzov P., et al., *Nuclear Instruments and Methods in Physics Research A*, 2020, vol. 958, p. 162154. https://doi.org/10.1016/j.nima.2019.04.108
7. Baldin A. A., Astakhov V. I., Beloborodov A. V., et al., *Proc. 27th Russ. Part. Accel. Conf. (RuPAC'21)*, 2021, p. 82. https://doi.org/10.18429/JACoW-RuPAC2021-WED05
8. Sandul V. S., Feofilov G.A., and Valiev F.F., *Physics of Particles and Nuclei Letters*, 2023, vol. 54, no. 4, p. 712. https://doi.org/10.1134/S1063779623040275
9. Galaktionov K.A., Roudnev V.A., and Valiev F.F., *Physics of Particles and Nuclei Letters*, 2023, vol. 54, no. 3, p. 446. https://doi.org/10.1134/s1063779623030152
10. Roudnev V.A., Galaktionov K.A., and Valiev F.F., *Bull. Russ. Acad. Sci. Phys.*, 2025, vol. 89. p. 1335. https://doi.org/10.1134/S1062873825712139
11. Galaktionov K.A., Roudnev V.A., and Valiev F.F., *Phys. Atom. Nuclei*, 2023, vol. 86, p. 1426. https://doi.org/10.1134/S1063778823060248
12. Galaktionov K.A., Roudnev V.A., and Valiev F.F*.,* *Moscow Univ. Phys.*, 2023, vol.78 (suppl 1), p. S52. https://doi.org/10.3103/S0027134923070081
13. Galaktionov K., Rudnev V., and Valiev F*., Phys. Part. Nuclei*, 2023, vol. 54, p. 446. https://doi.org/10.1134/s1063779623030152
14. Valiev F.F, Feofilov G.A., Tsvinev A.P., et al*., JINR Rapid Communications*, 1991, no 4/50/-91, p. 27.
15. Baldin A., Feofilov G., Gavrilov Yu., et al*., Nuclear Instruments and Methods in Physics Research A*, 1992, vol. 323, p.439. https://doi.org/10.1016/0168-9002(92)90329-3
16. Feofilov G, Kondratev V., Stolyarov O., et al*., Physics of Particles and Nuclei Letters*, 2017, vol. 14, no. 1, p. 150. https://doi.org/10.1134/S1547477117010125

FIGURE CAPTIONS

Fig. 1. Schematic diagram of the chevron-type MCP detector for charged particles.

Fig. 2. Typical current pulse from the MCP detector. Horizontal scale: 1 ns/div; vertical scale: 10 mV/div.

Fig. 3. Amplitude spectrum of signals from the MCP detector recorded during the detection of minimally ionizing particles (protons and pions with a momentum of 800 MeV$\cdot c^{-1}$) [14]. The arrows indicate the thresholds used in operation (*1* – 70 mV; *2* – 520 mV).

Fig. 4. Schematic diagram of the MCP chevron assembly with differential signal pickup.

Fig. 5. Low-background detector for minimally ionizing charged particles: *1* — registration unit; *2* — vacuum chamber; *3*, *10* — first and second chevron assemblies; *4*, *11* — flat anodes; *5*, *7*, *12*, *14* — signal transmission lines; *6*, *13* — vacuum connectors; *8*, *15* — fast comparators; *9* — nanosecond coincidence circuit.

FIGURES

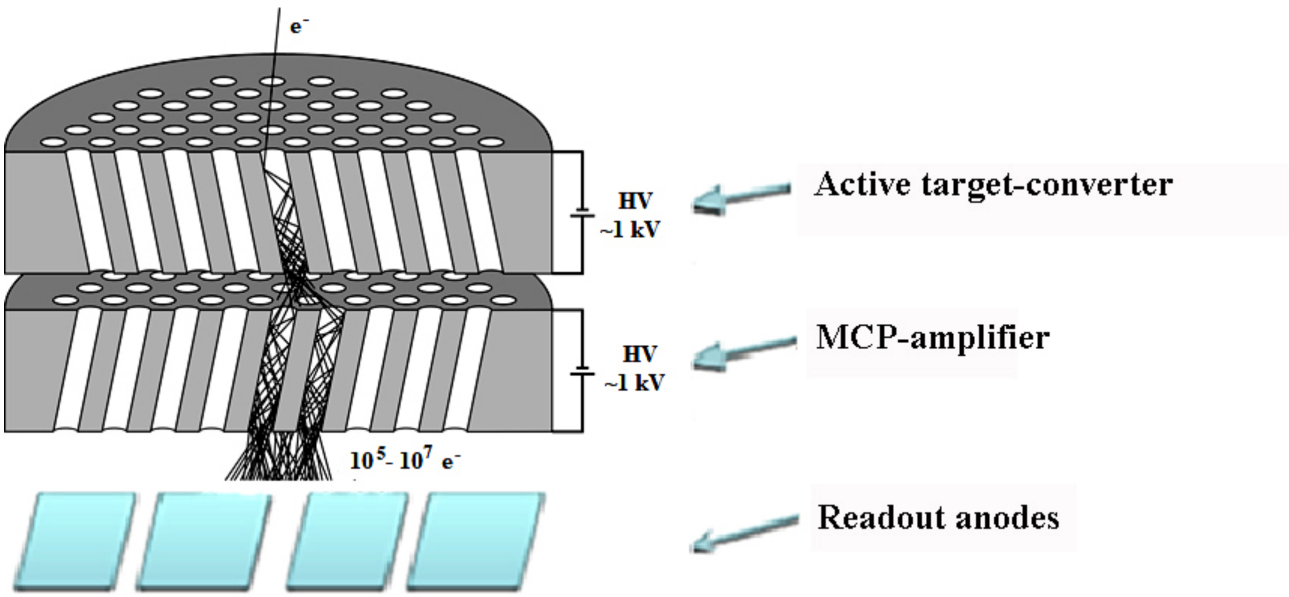

Fig. 1.

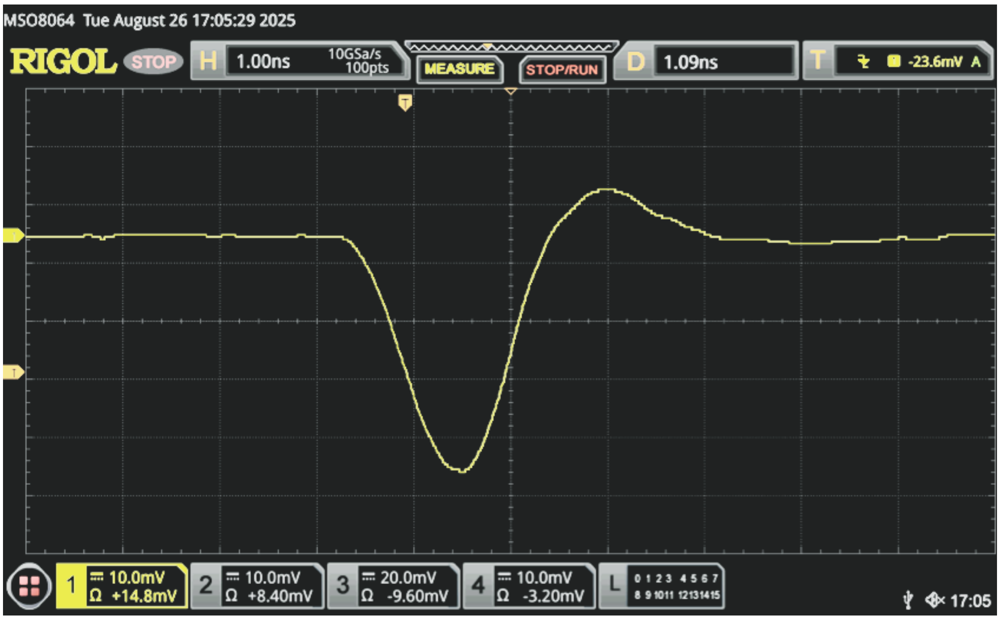
MSO8064 Tue August 26 17:05:29 2025
RIGOL
STOP
H
1.00ns
10GSa/s
100pts
MEASURE
STOP/RUN
D
1.09ns
T
-23.6mV
A
1
10.0mV
+14.8mV
2
10.0mV
+8.40mV
3
20.0mV
-9.60mV
4
10.0mV
-3.20mV
L
17:05

Fig. 2.

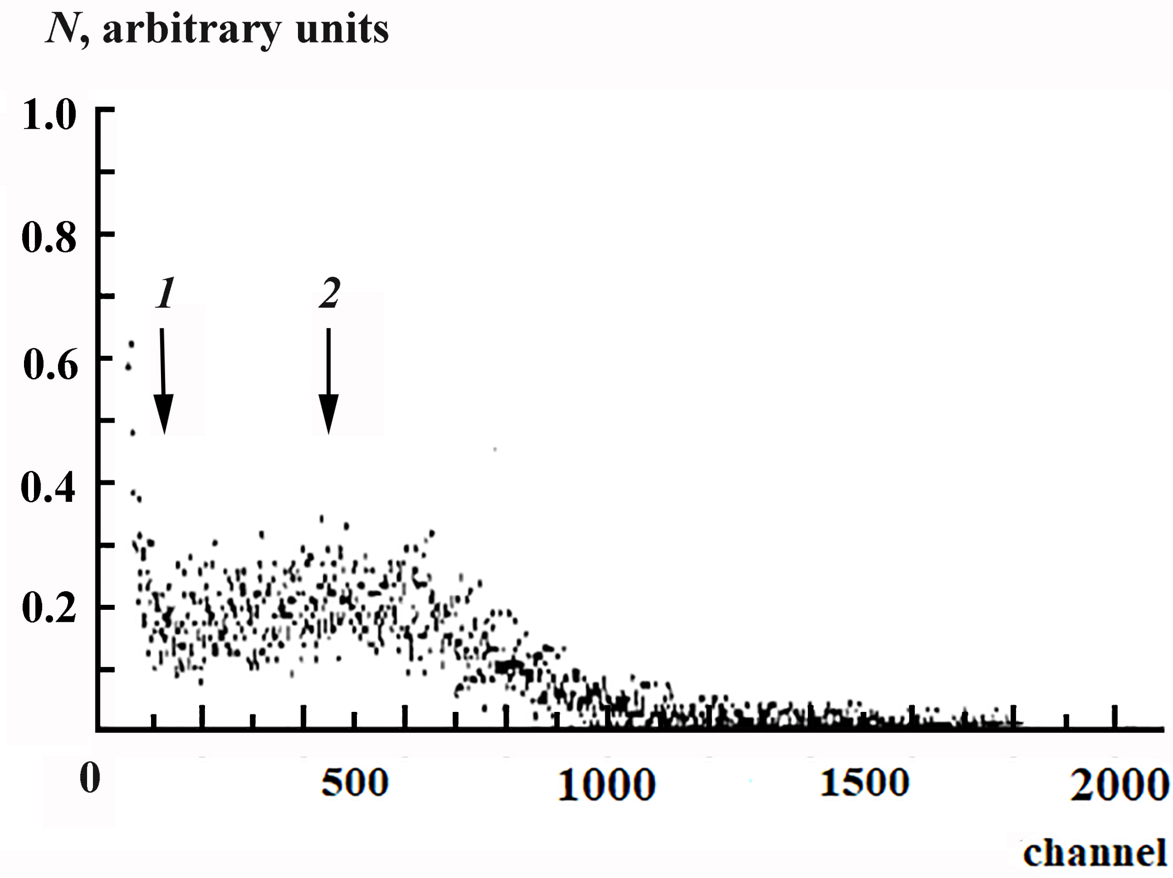

N, arbitrary units
1.0
0.8
0.6
0.4
0.2
1
2
0
500
1000
1500
2000
channel

Fig. 3.

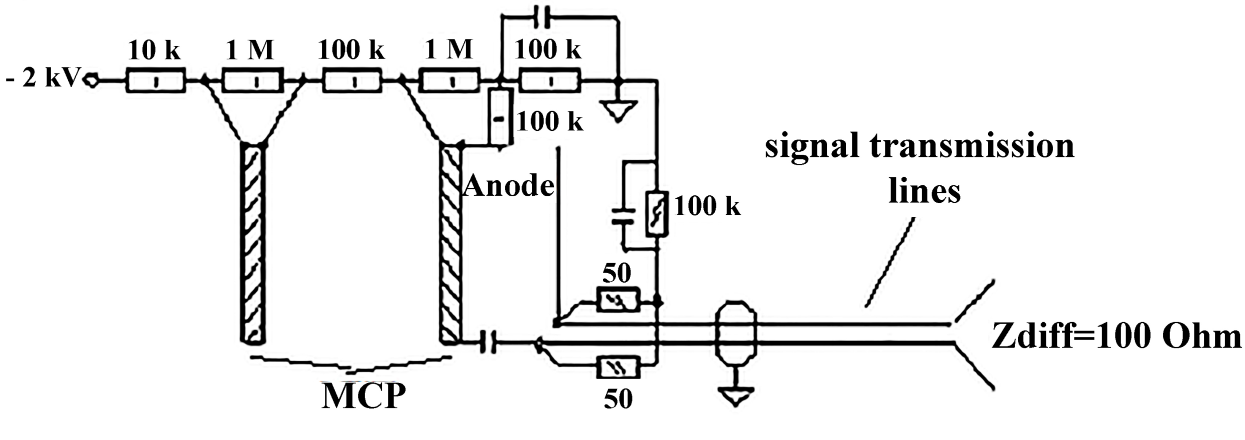
10 k
1 M
100 k
1 M
100 k
- 2 kV
100 k
Anode
100 k
50
50
MCP
signal transmission lines
Zdiff=100 Ohm

Fig. 4.

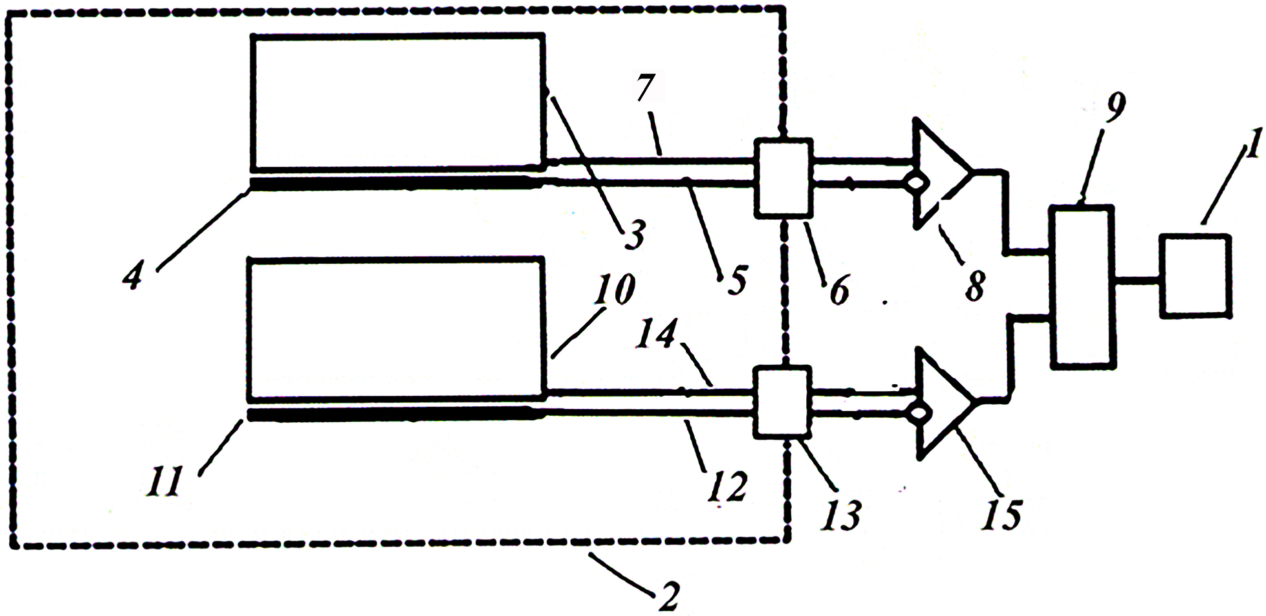

Fig. 5.